Light circulation and weaving in periodically patterned structures

David Crouse, Eric Jaquay, and Abdur Maikal
Department of Electrical Engineering, The City College of New York, 140th St. at Convent Ave., Steinman Hall, Room 614, New York, New York 10031, USA

Alastair P. Hibbins
Electromagnetic Materials Research Group, School of Physics, University of Exeter, Stocker Road, Exeter EX4 4QL, United Kingdom
(Received 19 December 2007; published 23 May 2008)

The circulation and weaving of light in one-dimensionally periodic structures as a result of the excitation of phase resonances are described. It is shown that phase resonances occur for *s*-polarized incident light with many similarities and some important differences compared to well-known *p*-polarized phase resonances. It is shown that surface plasmons are not necessary for either enhanced transmission or phase resonances to occur in one-dimensionally periodic slit arrays. Characteristics of phase resonances of both polarizations, including their production of a sharp minimum on the shoulder of a broader transmission peak are described by analyzing the power flow associated with these modes. Electromagnetic field intensities and phase difference in the coupled cavity modes that comprise phase resonances are discussed.

DOI: 10.1103/PhysRevB.77.195437 PACS number(s): 73.20.Mf, 42.25.Fx, 42.79.Dj, 71.45.Gm

Periodic metal-dielectric composite structures exhibit a number of anomalous optical characteristics, such as enhanced transmission, anomalous absorption, and phase resonances that have been studied for many years.[1–8] These periodic structures include transmission gratings, diffraction gratings, and more complicated one-dimensionally (1D) periodic metal-dielectric composites, all of which can be grouped under the label of plasmonic crystals. Numerous works have explained in detail the various optical and surface plasmon modes (SPs) that exist in these structures and their relative roles in producing the optical characteristics mentioned above.[9–12] Several works analyzed the relative roles of different types of SPs [i.e., horizontally oriented SPs (HSPs) on top and bottom air/metal interfaces, and coupled, vertically oriented SPs on the vertical walls of opposite sides of the grooves that undergo a Fabry-Perot resonance (VSP-CMs)] in producing enhanced transmission and absorption. Most of the works concluded that VSP-CMs, Rayleigh anomalies and waveguide modes are the modes primarily responsible for these phenomena in 1D transmission gratings, not HSPs.[10–12] In fact, it has now been shown both theoretically[5] and experimentally[12] that enhanced transmission occurs just as strongly in 1D transmission gratings with light polarized with the electric field oriented parallel to the surfaces of the metal wires (i.e., *s*-polarized light), a polarization that does not excite SPs. Most of the research on phase resonances has been done on 1D periodic transmission and diffraction gratings with light polarized with the magnetic field oriented parallel to the metal wires (i.e., *p*-polarized light).[6–8,13–15] Phase resonances for *p*-polarized incident light arise in 1D periodic structures that have multiple grooves per period (i.e., compound gratings). Many different types of compound grating structures support phase resonances including, but not limited to, compound gratings with the grooves within each period of the grating being identically composed and oriented except that not all the grooves are surrounded by the same identical configuration of neighboring grooves,[6] and, as described in this work, compound gratings with the grooves in each period that differ with respect to composition or dimensions. In these types of structures, *p*-polarized VSP-CMs in neighboring grooves couple to each other and produce field profiles of equal magnitude but with a π radians phase difference; such modes have come to be called π modes or π resonances.[6–8,14,15]

In this work, two tasks are performed: the first is to determine if a different type of cavity mode (CM) that is not produced by Fabry–Pérot resonances of SPs on the vertical walls of the grooves can produce π resonances, and the second is to study and describe the phenomenon of light circulation and light weaving that occurs when π modes are excited. This different type of CM is a simple wave guide cavity mode (denoted as WG-CM), whose energy is determined by both the height and width of the groove and the dielectric constant of the material filling the groove. WG-CMs do not involve surface plasmons and have a cutoff such that a minimum groove width is necessary to support them; such modes occur in 1D periodic transmission gratings with both *p*-polarized and *s*-polarized incident light.[5,12]

In Refs. 5, 12, and 16, all of the individual optical and surface plasmon modes that occur in 1D lamellar grating structures and their properties are described; we only list them below.

(1) Surface plasmons at the horizontally oriented metal/dielectric interfaces (HSPs);

(2) Surface plasmons at the vertically oriented metal/dielectric interfaces (VSPs), i.e., the walls of the grooves;

(3) Cavity modes within the grooves that are either pure waveguide modes (WG-CMs) or are produced by coupled VSPs on the walls of opposite sides of the grooves and that experience Fabry–Pérot resonance; such modes are denoted as VSP-CMs; and

(4) Rayleigh anomalies.

Combinations or hybrids of these modes can be formed, such as the coupling of two VSP-CMs in neighboring grooves to produce π resonances for *p*-polarized light incident on 1D transmission gratings.

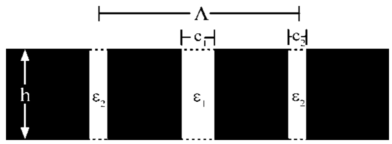

FIG. 1. Three groove structures are studied in this work. All the gratings have Au wires with a dielectric constant obtained from Ref. 17, $h=1$ μm and $\Lambda=3.5$ μm. Grating 1 is a single-groove-per-period grating with all the grooves being identical, with $\varepsilon_1=\varepsilon_2=23$ and $c_1=c_2=0.745$ μm; in this case, the period is reduced by half from what is indicated in the figure. Grating 2 is two-groove-per-period structure with $\varepsilon_1=\varepsilon_2=23$ and $c_1\neq c_2$, with $c_1=0.755$ μm and $c_2=0.735$ μm. Grating 3 is also a two-groove-per-period structure with $\varepsilon_1\neq\varepsilon_2$ and $c_1\neq c_2$ with $\varepsilon_1=25$, $\varepsilon_2=21$, $c_1=0.755$ μm, and $c_2=0.735$ μm. Grating 1 will exhibit dual polarization transmission, grating 2 (3) will have *s*-polarization (*p*-polarization) π resonances.

Many aspects of phase resonances in 1D gratings for *p*-polarized incident light were studied by Hibbins *et al.*,[13] in which they studied the π phase difference between the electric fields in neighboring grooves. They used finite-element modeling to numerically model all the optical, SP, and π modes and used a band-folding technique to provide a physical justification for the shape of the bands and the interactions between the modes. By analyzing the details of these π modes, they show that they are composed of coupled VSP-CMs in neighboring grooves.[13]

One issue that was not within the scope of Ref. 13 was whether such π resonances exist for *s*-polarized light. For *s*-polarized light, there is no component of the electric field that is normal to any metal/dielectric interface, and hence, SPs and VSP-CMs cannot be excited. However, WG-CMs do occur, and along with diffracted modes and Rayleigh anomalies are responsible for a large number of the enhanced or anomalous optical effects. As will be shown in this work, WG-CMs can couple with neighboring WG-CMs to produce *s*-polarized π resonances with properties similar to the properties of *p*-polarized π resonances. Consider the three grating structures described in Fig. 1 and its caption. These three gratings exhibit many enhanced and anomalous optical characteristics for both *p*-polarized and *s*-polarized incident light. The first grating that will be studied, which is denoted as grating 1, has identical grooves with widths $c=0.745$ μm, heights $h=1$ μm, dielectric constants $\varepsilon=23$, a period $\Lambda=1.75$ μm, gold for the wires (dielectric constant obtained from Ref. 17), and air as the superstrate (i.e., top layer) and substrate. As is shown in Fig. 2, this structure exhibits enhanced transmission for both *s*-polarized and *p*-polarized $\lambda=5$ μm (0.248 eV) normal incidence light. Besides being yet another example of enhanced transmission for *p*-polarization, a phenomenon that has been extensively described in the literature, this structure exhibits enhanced transmission for *s*-polarized light produced by an excited WG-CM. A systematic four-step procedure to design a grating with the appropriate period, height, groove dimensions, and all other parameters to achieve simultaneous enhanced transmission for *s*-polarized and *p*-polarized lights at a particular wavelength is described in detail in Ref. 12 (and to a lesser extent in Ref. 5) along with a detailed discussion of the mechanisms responsible for enhanced transmission for *s*-polarized incident light and more examples of electromagnetic field profiles and Poynting vector profiles in both Refs. 5 and 12. This procedure is (step 1) choose a period for the grating that is smaller than the wavelength of interest to avoid the onset of any diffraction, (step 2) choose values for c, h, and $\varepsilon_{\mathrm{groove}}$ to get *s*-polarized and *p*-polarized WG-CMs in the approximate wavelength range desired, (step 3) vary h to get the *p*-polarized WG-CM to the desired wavelength, and finally (step 4) vary c to get the *s*-polarized WG-CM to desired wavelength. Note that with this procedure, because of the cut-off frequency for *s*-polarized WG-CMs, a material with a large dielectric constant is needed to be placed in the groove so that the groove width can be made smaller than the free-space wavelength of the WG-CM and substantially smaller than the period of the grating; also note that the *p*-polarized WG-CMs will have little dependence on c as explained in Refs. 5 and 12.

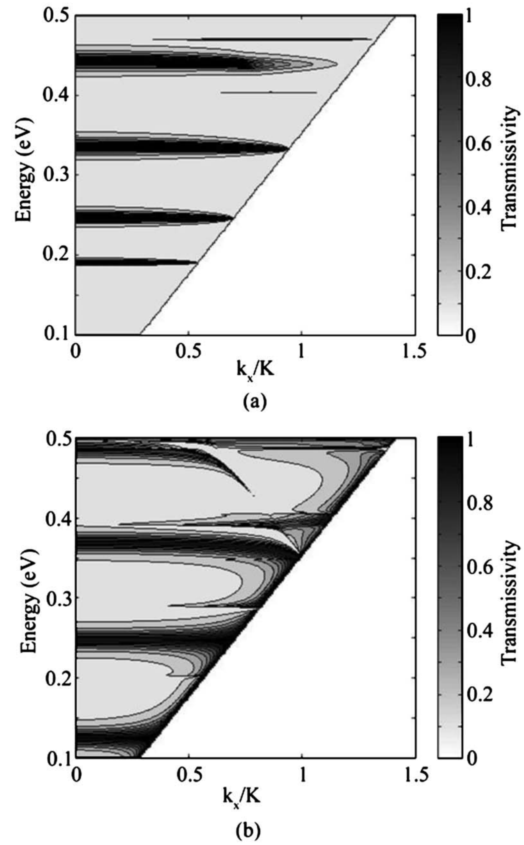

FIG. 2. The transmissivitty for (a) *s*-polarized incident light and (b) *p*-polarized incident light for grating 1 (grating parameters are given in Fig. 1). K is $2\pi/\Lambda$, where $\Lambda=3.5$ μm. The period Λ is deliberately chosen as twice as large as in the one-groove-per-period grating in anticipation of perturbing the width of every other groove to produce a two-groove-per-period grating with twice the period later in this work.

Now, consider if the widths of every *other* groove are perturbed to have widths of $c_1=0.755$ μm and the widths of the rest of the grooves perturbed to have widths of $c_2=0.735$ μm, while the rest of the grating parameters are unchanged. The resulting structure is the two-groove-per-period grating (grating 2 of Fig. 1) and can be considered as being composed of the convolution of two gratings, a long period grating with $\Lambda_1=3.5$ μm, and a short period grating with $\Lambda_2=1.75$ μm. The band folding techniques described in Refs. 8 and 13 can be used to construct the approximate shapes of the *p*-polarization and *s*-polarization photonic and plasmonic bands. This band folding technique involves starting with the photonic band structure for a simple short-pitch grating with all the grooves being identical, then applying a perturbation to every second, third or some higher number groove resulting in a long pitch perturbative component to the structure. This long pitch perturbative component is convoluted in a straightforward manner (as described in Refs. 8 and 13) into the photonic band structure defined by the short pitch of the original unperturbed grating. The effects of this convolution of the long and short pitch components of the photonic band structure, including the presence of new light lines, CM-HSP mode repulsion and hybridization (i.e., the CMs acquire more dispersion and HSP characteristics as they approach, in terms of energy and momentum, the light lines) are clearly present for the *p*-polarized photonic band structure shown in Fig. 3(b) but much less so in the *s*-polarization photonic band structure shown in Fig. 3(a). While the band-folding procedure is certainly applicable to the *s*-polarization band structure, because there are no surface plasmons for *s*-polarized incident light and only low dispersion WG-CM bands, it is sufficient to consider that the two slightly different grooves will have slightly different resonant frequencies, causing each WG-CM band to split into two bands that may interact. Figure 3(a) shows the full *s*-polarized photonic band structure and shows that almost every *s*-polarized CM band of grating 1 [Fig. 2(a)] is the split into two CM bands separated by an *s*-polarized π resonance. For $k_x=0$, *s*-polarized π resonances are clearly seen to occur at energies of 0.192, 0.248, and 0.334 eV and *p*-polarized π resonances are clearly seen to occur at energies of 0.121, and 0.24 eV. Also, additional diffraction modes and their associated light lines and CM-diffraction interactions are produced. Many similarities and several important differences between *s*-polarized and *p*-polarized π resonances are seen to exist. First, Fig. 3(b) shows an *s*-polarized π resonance with a π radian difference in the phase of $\mathbf{H}$ in neighboring grooves that is similar to the π radian difference in the phase of $\mathbf{E}$ for *p*-polarized π resonances. One difference between *s*-polarized and *p*-polarized π resonances is that near the light lines, the dispersion of all the *s*-polarization bands, including the π resonances, are far less than the dispersion of *p*-polarized photonic bands near the light lines [see Figs. 3(a) and 3(c)]. Another important and obvious difference between the *s*-polarized and *p*-polarized π resonances is that *s*-polarized π resonances are necessarily produced by coupled WG-CMs because of the absence of SPs in *s*-polarization.

It is argued in Ref. 13 that direct coupling of the incident beam with π resonances cannot occur because the field in half the grooves is π radians out of phase with the incident beam. Hence, the π resonances should always be located on the shoulders of the broad transmission peak. We have observed in numerous two-groove-per-period gratings that the *s*-polarized π resonances tend to be closer to the center of the transmission peak than the *p*-polarized π resonances. This property arises because of the different constituent components that make up the *s*-polarized and *p*-polarized π resonances. For *p*-polarized π resonances, on the high energy side of the π resonance transmission minimum, there exists a broad (i.e., low *Q* or highly radiative) VSP-CM transmission peak. This peak is located at approximately the same energy value as the peak which existed prior to the additional band

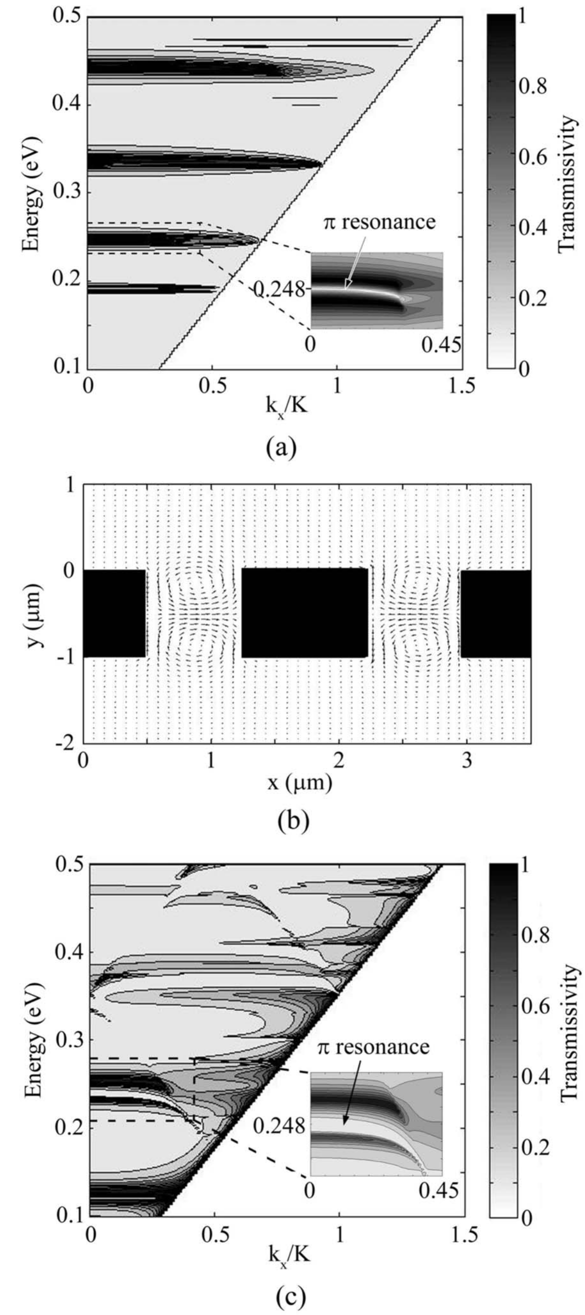

FIG. 3. (a) The transmissivity for *s*-polarized incident light on grating 2. (b) The orientation of $\mathbf{H}$ for the *s*-polarized 0.248 eV; $k_x=0$ π resonance in grating 2 shows the π phase difference of $\mathbf{H}$ in neighboring grooves. (c) The transmissivity for *p*-polarized incident light on grating 3. The insets show the π resonance, showing that the broad transmission bands now have transmission minima on the shoulder of the bands.

folding required by the perturbation induced by the convolution of the long period grating. On the low energy side of the p-polarized π resonances, the transmission peak is produced by a SP band that was initially outside the light cone and has been folded into the light cone by the long period grating perturbation at slightly lower energies than the low-Q VSP-CM band. Hence this lower energy, band folded SP band is inherently less radiative, resulting in a higher Q. This low-Q/high-Q pair of transmission peaks creates an asymmetric transmissivity curve for the p-polarized π resonance. For s-polarized π resonances, the band folding technique is not necessary for several reasons, one being that there are never any SP bands or other modes outside the light cone into which they would be folded by a long period perturbation; all the s-polarized WG-CMs can interact with incident or radiating light. Breaking the symmetry of the grooves (i.e., making them different in some way either by perturbing the widths or heights of the grooves, or by perturbing the dielectric constant of the material filling one groove relative to the dielectric constant of the material filling the other grooves within one period of a compound grating, or by perturbing the environment surrounding one groove relative to the environment that surrounds the other grooves within one period of a compound grating) simply splits the original WG-CMs bands into two bands with some asymmetry (the π resonance still has to occur on the shoulder of the original WG-CM transmission peak), but typically being more symmetrical than the two VSP-CMs bands for a p-polarization π resonance. This s-polarized WG-CM band splitting produces two WG-CMs with similar Q values and a more symmetric transmissivity curve (relative to p polarization) about a s-polarized π resonance. This property also affects the nature of the power flow on either side of π resonance and is discussed later in this paper.

To produce p-polarized π resonances, either substantially larger relative differences in the groove width are necessary, as is done in Ref. 13, or one can change the groove height or dielectric constant of the material filling the grooves,[7] as is done in this work. This is because the p-polarized π resonances are composed of interacting p-polarized VSP-CMs, whose energies have small dependences on the widths of the grooves (relative to the energies of s-polarized WG-CMs); an example of these dependencies of CM energies on groove widths is shown in Fig. 3 of Ref. 5. However, the energies of the constituent VSP-CMs of a p-polarized π resonance have strong dependencies on groove height and the dielectric constant of the material filling the groove;[5,16] therefore, perturbations in these two parameters can be used to produce p-polarized π resonances. Starting with grating 2 with $c_1=0.755\ \mu\text{m}$, $c_2=0.735\ \mu\text{m}$, and $\varepsilon_1=\varepsilon_2=23$, then perturbing ε_1 and ε_2 such that $\varepsilon_1=25$ and $\varepsilon_2=21$ to arrive at grating 3 in our work, a grating that supports p-polarized π resonances [Fig. 3(b)] that are similar to the ones studied in past works on p-polarized π resonances.[6–8,14,15] The reader is referred to these works[6–8,14,15] for the description of the numerous properties of p-polarized π resonances. The rest of this work involves an aspect heretofore not discussed or analyzed in detail, namely, light circulation and light weaving properties of s-polarized and p-polarized π resonances.

If instead of looking at the phase of the magnetic or electric field in the grooves when a π resonance is excited but rather the power flow, as shown by the Poynting vector, one sees that at and around the transmission minimum (reflection maximum) produced by π resonances, light is transmitted with high transmissivity through the two sets of grooves but then curves, or circles around, and is transmitted with high transmissivity through the neighboring grooves, resulting in a reflection maximum. It is evident that π resonances are hybrid modes, composed of two coupled VSP-CMs or WG-CMs for p-polarized light, or two coupled WG-CMs for s-polarized light. Furthermore, at the transmission minimum, these two transmission channels created by the two coupled CMs are equal in magnitude but produce counter propagating circulations of light resulting in high field intensities in the grooves but a net zero power flow in the grooves as equal amounts of power flow up and down the groove. Figures 4(a) and 4(b) show the Poynting vector profiles for s-polarized light at wavelengths slightly larger and smaller than the wavelength of the transmission minimum respectively. Two things seem to be occurring on either side of the π resonance transmission minima to degrees that vary depending on whether it is a p-polarized or s-polarized π resonance and involve a competition between the two transmission channels produced by the two coupled CMs in neighboring grooves. Immediate on either side of the more symmetric s-polarized π resonance transmission minima, one transmission channel associated with one set of grooves becomes weaker than the other transmission channel associated with the other set of grooves. Thus, of the two transmission channels that are presented to incident light, larger amounts of power are trans-

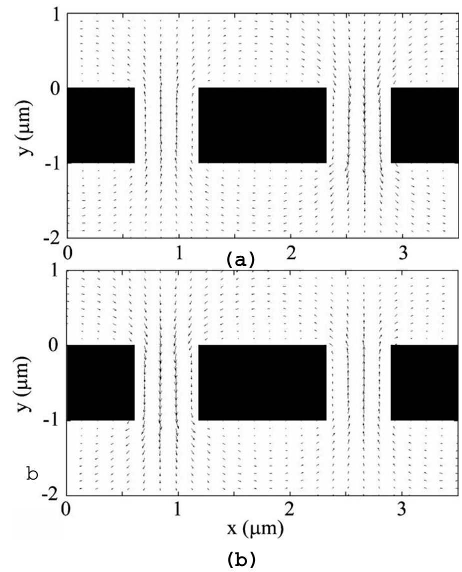

FIG. 4. For s-polarized normal incident light on grating 2, we have (a) the Poynting vector profile on the low energy side of the π resonance (i.e., $\hbar\omega=0.2479$ eV). The power flowing down through the left groove is decreasing and not totally offsetting the circulating power flowing down through the right groove and up through the left groove. (b) For an energy slightly larger than the π resonance (i.e., $\hbar\omega=0.2484$ eV), the opposite situation occurs where the power flowing down through the right groove is decreasing and not totally offsetting the circulating power flowing down through the left groove and up through the right groove.

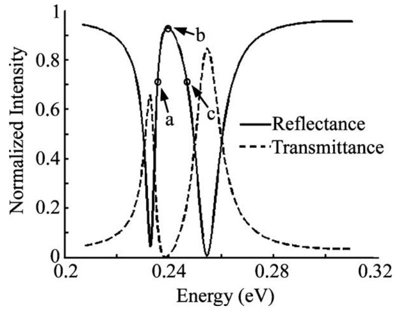

FIG. 5. The reflectivity and transmissivity for *p*-polarized normal incident light on grating 3. The *p*-polarized π resonance with an energy of 0.239 eV exhibits strong light circulation only on the low energy side of the peak, as shown in Fig. 6.

mitted through the stronger transmission channel (i.e., one set of grooves) relative to the weaker transmission channel (i.e., the other set of grooves). However, the weaker transmission channel is still strong enough to present to the now transmitted light on the substrate side, a strong and viable transmission channel back through the grating. The net result of this process is a high reflectance. For energies progressively further from the π resonance transmission minimum, the weaker transmission channel retransmits progressively lesser amounts of light, which had been transmitted to the substrate via the stronger transmission channel, resulting is decreasing light circulation and increasing transmissivity.

For *p*-polarized π resonances a different situation occurs, a difference produced by the asymmetric nature of the transmission minimum and maxima that make up the *p*-polarized π resonances, as discussed earlier. As shown in Figs. 5 and 6, starting well on the higher energy side of the transmission minimum (or reflectance maximum) (point *c* in Fig. 5), the high-Q, lower energy VSP-CM constitutes the weaker transmission channel at these energies and is only weakly excited and does not transmit or retransmit much light [Fig. 6(c)]. The low-Q, higher energy VSP-CM constitutes the stronger transmission channel and becomes progressively weaker as the energy approaches the energy of the transmission minimum, resulting in progressively less transmission. On the other side of the transmission minimum (i.e., the low energy side or point *a* in Fig. 5), the VSP-CMs in both channels are still strong, but not equal, resulting in strong light circulation [Fig. 6(a)]. These types of π resonances are characterized by a difference in energy between the absorption maximum and transmission minimum.[13] It is argued that the absorption maximum is the true location of the π resonance because it is at this energy that the intensities of the fields of the CMs within the grooves, on average or taken collectively, are largest.

For these *p*-polarized and *s*-polarized π resonances, the effects of absorption can be anticipated by considering the effects of absorption on the constituent CMs of π resonances. When a *p*-polarized or *s*-polarized CM is excited, a strong intensification of the field strength within the slits occurs resulting is in a corresponding increase in absorption.[5,13] An effect of absorption is that power is transferred from the fields to the lossy metal or other materials in the structure, lowering the transmittance of CMs and subse-

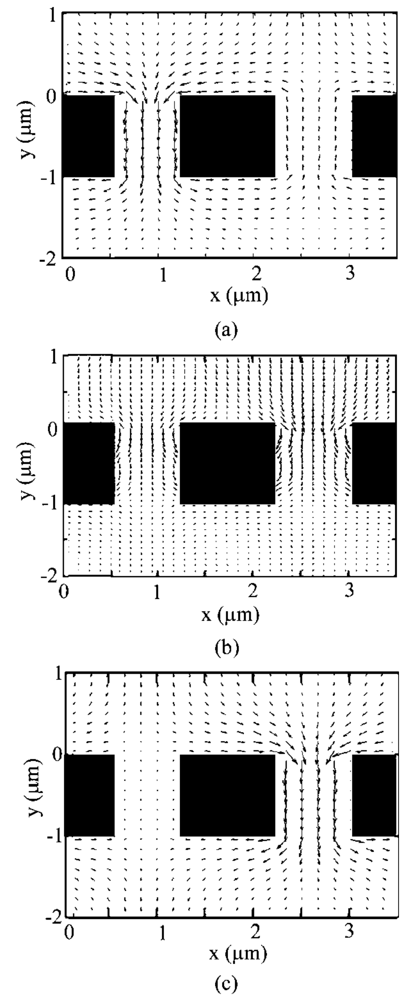

FIG. 6. The Poynting vector profiles for *p*-polarized normal incident light with energies (a) 0.236 eV that is slightly below the π resonance (point a in Fig. 5), (b) 0.239 eV that is the peak in reflectance of the π resonance (point b in Fig. 5), and (c) 0.246 eV that is slightly above the π resonance (point c in Fig. 5). At the peak of reflectance of the π resonance [see (b)], the counterpropagating light circulations largely offset each other in terms of power flow in the grooves. The small amount of power flowing into the two grooves flows into the walls of the groove and is absorbed by the lossy gold wires. For energies slightly less than the peak [see (a)], the high-Q CM in the left-hand groove dominates but the higher energy low-Q CM of the right-hand groove can still present to the light transmitted through the left-hand groove with a strong transmission channel back through to grating, resulting in light circulation. For energies slightly less than the peak [see (c)], the low-Q CM in the right-hand groove dominates but the CM of the left-hand groove generally has too high of a Q to present to the light transmitted through the right-hand groove a strong transmission channel. Hence, little light circulation is observed on this high energy side of the π resonance reflectance peak.

quently lowering the reflectance peaks of the π resonances described in this work. Also, as described in Ref. 5, the intensity of the fields of a *p*-polarized VSP-CM is large on the walls of the groove (and correspondingly large in the metal near the walls of the grooves) as opposed to *s*-polarized WG-CMs, in which the intensity of the fields is concentrated in

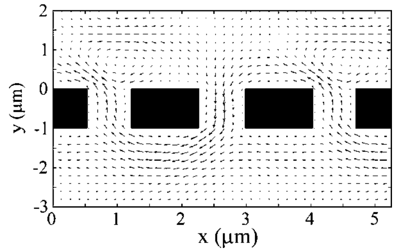

FIG. 7. For s-polarized, 0.24815 eV light, incident on grating 2 at a 15° angle of incidence, the π resonance causes light to weave up and down through the grooves with a net power flow in the $\hat{x}$ direction.

the middle of the grooves. Hence, a grating structure with a lossy metal will diminish the p-polarized VSP-CMs and π resonances more than the s-polarized WG-CMs and π resonances, whereas a grating structure with a lossy dielectric material filling the grooves will diminish the s-polarized WG-CMs and π resonances more than the p-polarized VSP-CMs and π resonances.

For off-normal incident angle, this light circulation turns into light weaving as the light weaves its way back and forth through the structure while having a net power flow in one direction (Fig. 7). Numerous other structures can be designed with more than two grooves per period, or with multiple layers of gratings, in which light weaves and circulates around the metal wires in increasingly complex ways.

Besides the importance of verifying that π resonances occur for s-polarized light and describing light circulation and weaving, there are a wide range of potential applications in which these π resonances can be used or should be avoided. These applications range from relatively simple polarizers and wavelength filters to more exotic applications where the flow of light is controlled, slowed or trapped in circulating or surface modes. An example of an application where s-polarized π resonances should be avoided is a polarizer that makes use of enhanced transmission of s-polarized light. In practical device fabrication, the actual groove width of any one groove may vary somewhat from the width of its neighbors. This will produce a π resonance that will reduce the transmissivity for s-polarized light through those two grooves and thus the transmissivity of the overall structure. We have found that for structures similar to the ones studied in this paper, groove width variations of only one-third of 1% can produce s-polarized π resonances and transmission minima where maxima were expected. Therefore, unless the groove widths vary by less than this amount, π resonances will be excited in a large number of groove pairs that will greatly reduce the transmissivity. However, we have found that some s-polarized transmission peaks are more stable than others with respect to variations in groove width. Hence, if a particular s-polarization transmission peak is going to be used in a device, a "stability analysis" of that peak should be performed to determine if it will remain highly transmitting upon reduction to practice.

In conclusion, this work has shown that π resonances occur for s-polarized incident light and have properties similar to those of p-polarized π resonances. Such properties include a sharp transmission minimum on the shoulder of a broader transmission maximum, light circulation, and light weaving. These π resonances are produced by coupled cavity modes in neighboring grooves with slightly different compositions or orientations. Light circulation and weaving produced by π resonances has been described, in which light is transmitted through the structure, then circulates around to neighboring grooves and is retransmitted through the structure.

D.C. would like to acknowledge financial support of the Cornell Center for Nanoscale Systems in Information Technologies. Alastair Hibbins would like to acknowledge the financial support of the Engineering and Physical Sciences Research Council (EPSRC, UK).

[1] R. W. Wood, Philos. Mag. **4**, 396 (1902).
[2] T. W. Ebbesen, H. J. Lezec, H. F. Ghaemi, T. Thio, and P. A. Wolff, Nature (London) **391**, 667 (1998).
[3] A. Barbara, P. Quemerais, E. Bustarret, and T. Lopez-Rios, Phys. Rev. B **66**, 161403(R) (2002).
[4] E. Popov and L. Tsonev, Opt. Commun. **69**, 193 (1989).
[5] D. Crouse and P. Keshavareddy, Opt. Express **15**, 1415 (2007).
[6] Diana C. Skigin and Ricardo A. Depine, Phys. Rev. E **74**, 046606 (2006).
[7] Diana C. Skigin, Hung Loui, Zoya Popovic, and Edward F. Kuester, Phys. Rev. E **76**, 016604 (2007).
[8] Y. G. Ma, X. S. Rao, G. F. Zhang, and C. K. Ong, Phys. Rev. B **76**, 085413 (2007).
[9] J. A. Porto, F. J. Garcia-Vidal, and J. B. Pendry, Phys. Rev. Lett. **83**, 2845 (1999).
[10] Qing Cao and Philippe Lalanne, Phys. Rev. Lett. **88**, 057403 (2002).
[11] David Crouse and Pavan Keshavareddy, Opt. Express **13**, 7760 (2005).
[12] David Crouse, Alastair Hibbins, and Matthew J. Lockyear, J. Appl. Phys. (to be published).
[13] Alastair P. Hibbins, Ian R. Hooper, Matthew J. Lockyear, and J. R. Sambles, Phys. Rev. Lett. **96**, 257402 (2006).
[14] A. N. Fantino, S. I. Grosz, and D. C. Skigin, Phys. Rev. E **64**, 016605 (2001).
[15] D. C. Skigin and R. A. Depine, Phys. Rev. Lett. **95**, 217402 (2005).
[16] D. Crouse, IEEE Trans. Electron Devices **52**, 2365 (2005).
[17] *Handbook of Chemistry and Physics*, edited by David R. Lide (CRC, London, 1993), pp. 10–1.